Proceedings Paper:
Du, W., Liu, Y., Tang, N. et al. (2025) Energy consumption minimization of air-to-water visible light communications. In: 2025 IEEE International Conference on Communications Workshops (ICC Workshops). 2025 IEEE International Conference on Communications Workshops (ICC Workshops), 08-12 Jun 2025, Montreal, Canada. Institute of Electrical and Electronics Engineers (IEEE), pp. 2057-2062. ISSN: 1938-1883. EISSN: 1550-3607.

https://doi.org/10.1109/ICCWorkshops67674.2025.11162473

Energy Consumption Minimization of Air-to-Water Visible Light Communications

Wenzhi Du, Yang Liu, Na Tang, *Member, IEEE*, and Xiaoli Chu, *Senior Member, IEEE*

***Abstract*—As offshore industries and the Internet of Underwater Things (IoUT) continue to expand, air-to-water communication is needed to connect various underwater sensors and things to the outside world. Visible light communication (VLC) has the potential to provide higher data rates and longer transmission distances than radio frequency and other air-to-water communication techniques. This paper presents an air-to-water VLC system where a light emitting diode (LED) transmitter carried by a hovering unmanned aerial vehicle (UAV) transmits data to an underwater receiver. We minimize the UAV energy consumption that includes both LED transmission and UAV propulsion energy consumption by optimizing the LED transmit power while guaranteeing that the average received signal-to-noise ratio (SNR) at the underwater receiver is above the required SNR. A sequential quadratic programming (SQP)-based algorithm is proposed to solve this problem. Simulation results show that our optimized LED transmit power reduces the total UAV energy consumption by up to 45% as compared to the benchmark schemes without increasing the transmission time for a given data volume.**

***Index Terms*—Air-to-water, energy consumption, UAV, visible light communication**

I. Introduction

Owing to growing underwater activities, e.g., undersea oil & gas exploration, and the Internet of Underwater Things (IoUT) [1], which are expected to connect the outside world to various underwater nodes, sensors and autonomous underwater vehicles, energy-efficient air-to-water wireless communications are urgently needed by the industry, military, and scientific communities. Traditionally, the communication between air and underwater requires that receives radio frequency (RF) signals from a transmitter above water and transmits acoustic [2] or optical signals [3] to an underwater receiver, but this solution can be costly since it requires a boat or a buoy that is equipped with both radio and acoustic/optical modems.

Some researchers have recently started to study air-water communications without using a relay. In [4], water-to-air communication was realized by deploying a high-frequency radar 20 to 40 cm above water to decode the vibrations on the water surface caused by sonar signals sent from an acoustic transmitter in a water tank, but the system does not support air-to-water transmissions. Sangeetha et al. [5] used a 635 nm 4.8 mW laser diode (placed beneath a glass water tank filled with water of 0.3 m depth) to transmit to a silicon photodetector (located 0.5 meter above the water), and achieved a bit error rate (BER) of 10^{-3} at a baud rate of up to 110 Kbps. However, laser light transmission has a very high directivity and requires the transmitter and receiver to be precisely aligned, which is difficult to realize in practical air-to-water communications.

Visible light communication (VLC) has also been considered for air-to-water communications, which will have the potential to support a variety of applications, such as air-water search and rescue, underwater sensor networks and underwater resource exploration [6]. Compared with acoustic and RF communications, VLC has higher bandwidth and lower energy consumption, so it can achieve a higher data rate for air-water communication [6]. Although the communication range of VLC is typically limited to below 50 meters underwater [7], it can provide a sufficiently large coverage via diffuse light transmission, e.g., by using light emitting diodes (LEDs).

In [8], three collinear LEDs were used to increase the VLC underwater coverage area and the received signal strength under turbid water conditions, but the noise or the air-to-water VLC channel effects is not considered and there was no information about how the LEDs were held above the water, and thus the associated energy consumption was not considered. Although the idea of rotating the cross section to extend the analysis of underwater VLC coverage to 3D was mentioned in [8], there was no mathematical model or expression of the rotated water surface elevation function. The air-to-water VLC link gain was experimentally investigated with a green LED at 75 cm above the water transmitting to a receiver 10 cm beneath the water in a water tank under the ambient light simulated by a white LED [9]. However, the turbidity of water is low in the water tank, and only the link gain is considered as the performance parameter.

We note that air-to-water VLC is still facing some critical challenges that need to be tackled. Firstly, the water surface is often wavy and time-varying, which affects the proportion of light that passes through the air-water interface due to reflection and the underwater propagation path due to refraction, thus affecting the transmission distance and underwater coverage area. Secondly, there are various underwater noise sources, which may degrade the signal-to-noise ratio (SNR) and channel capacity. Thirdly, the required LED transmission power increases with the depth of the underwater receiver and the attenuation coefficient of water for achieving a certain communication performance, while the unmanned aerial vehicle (UAV) that carries the LED transmitter is typically energy limited.

This work was supported in part by the UK EPSRC under grant EP/X021211/1 and the European Union's Horizon 2020 research and innovation program under grant agreement No. 898893.

Wenzhi Du, Na Tang, and Xiaoli Chu are with School of Electrical and Electronic Engineering, The University of Sheffield, Sheffield S1 4ET, UK. Yang Liu is with Nokia Bell Labs, Cambridge, UK. (e-mail: wenzhi9009@163.com; yang.16.liu@nokia.com; na.tang@sheffield.ac.uk; x.chu@sheffield.ac.uk).

In this paper, we study low-power air-to-water communications while considering that the underwater receiver may be drifted by water currents within a certain range from its default position. Hence, we choose LEDs as they can emit light in more diffused beams (resulting in larger coverage areas) with lower transmission power than lasers. More specifically, we consider an air-to-water VLC system, where a LED transmitter carried by a UAV hovering above water transmits a certain volume of data to an underwater receiver. Based on the widely used intensity modulation/direct detection (IM/DD) scheme, we adopt an on-off keying (OOK) non-return-to-zero (NRZ) modulation for the VLC link. We propose an algorithm to minimize the total energy consumption of the UAV by optimizing the LED transmit power while guaranteeing that the average received SNR at the underwater receiver is above the required SNR. The contributions of this paper are summarized as follows:

- We model the potentially wavy water surface by using Stokes's third-order theory [10] and analytically derive the light incident point on the water surface for a given UAV position and all possible positions of the underwater receiver that fall inside the light coverage. Based on this model, the transmission distance above and under water and the angle between the light propagation direction and the optical axis of the receiver are obtained. Furthermore, we present the water surface elevation function in the rotated cross sections so that the VLC underwater coverage can be analyzed in 3D.
- We use the models of the water surface and light propagation path to derive the SNR at the underwater receiver and the channel capacity for OOK-NRZ while considering the transmittance, the receiving area and the underwater noise terms. Based on our derived expressions of the received SNR and the channel capacity, we calculate the time required for the UAV-carried LED transmitter to transmit a given amount of data to the underwater receiver and the UAV energy consumption that includes both the energy used for VLC by the LED transmitter and the UAV propulsion energy consumption when hovering above the water at a given position.
- Leveraging the above analytical results, we formulate a problem to minimize the UAV energy consumption for transmitting a certain volume of data to an underwater receiver at a given depth by optimizing the LED transmit power while ensuring the received SNR is sufficient for a target BER. We solve the UAV energy consumption minimization problem by exploiting the trade-off between saving LED transmission power and saving UAV propulsion energy, e.g., reducing the LED transmit power increases the required data transmission time and leads to a higher UAV propulsion energy consumption. We devise a sequential quadratic programming (SQP)-based algorithm to numerically solve the optimization problem.
- Simulation results show that the optimized LED transmit power obtained by our proposed algorithm can reduce the UAV energy consumption by around 45% for the underwater receiver depth of 10 meters as compared to the benchmark schemes, without increasing the transmission time for transmitting a certain data volume.

The rest of this paper is organized as follows. In Section II, we present the system model for air-to-water VLC. The UAV energy consumption minimization problem is formulated and solved in Section III. Section IV presents the simulation results. The paper is concluded in Section V.

II. System Model

We consider an air-to-water VLC system, where a UAV carrying a LED transmitter hovers above the water and sends VLC signals to an underwater receiver. Since light in the blue-green wavelength range between 450-570 nm has the minimum absorption and scattering coefficients in water among all optical wavelength ranges [8], we choose a LED transmitter that has a dominant wavelength in this range. The receiver is located less than 20 meters beneath the water surface.

A. Water Surface Model

The cross section of an air-to-water communication environment at a given time instant is plotted in the (x, y) plane in Fig. 1. According to Stokes's third-order theory [10], the water surface elevation can be expressed as follows:

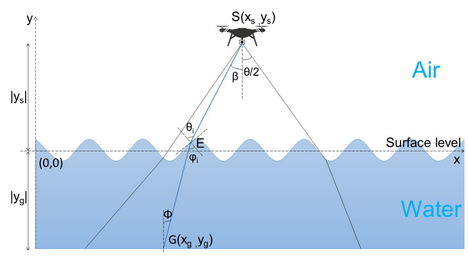

Fig. 1. A cross section of the air-water interface.

$$
\begin{aligned}
f(x,t) =& \alpha \left\{ \left[1 - \frac{1}{16}(k\alpha)^2 \right] \cos(kx - \omega t) \right. \\
&+ \frac{1}{2}(k\alpha) \cos\left[2(kx - \omega t)\right] \\
&\left. + \frac{3}{8}(k\alpha)^2 \cos\left[3(kx-\omega t)\right] \right\} + O\left[(k\alpha)^4\right], \quad (1)
\end{aligned}
$$

$$k = \frac{2\pi}{\lambda_w}, \quad (1a)$$

$$\omega = k \left[1 + \frac{1}{2}(k\alpha)^2 \right] \sqrt{\frac{g}{k} + O\left((k\alpha)^4\right)}, \quad (1b)$$

where x is the horizontal coordinate of a point on the water surface, t is time, ω is the angular frequency of the water wave, α is the first-order wave amplitude, k is the angular wavenumber, $k\alpha$ is the wave steepness, $O((k\alpha)^4)$ is the sum of least significant terms, λ_w denotes the wavelength of water waves, and g is the gravitational acceleration. The time period T_w of the water wave is given by:

$$T_w = 2\pi/\omega. \quad (2)$$

B. Light Propagation Path

For analytical tractability, we assume that the LED transmitter points downward vertically and the underwater receiver points upward vertically. Denote the positions of the LED transmitter and the underwater receiver in the (x, y) plane by $S(x_s, y_s)$ and $G(x_g, y_g)$, respectively. The UAV knows the default position of the underwater receiver at (x_s, y_g) and hovers straight above it, but the underwater receiver may be drifted away from its default position by the water current. We assume that the underwater receiver is kept within a radius of x_0 from its default position at the water depth $|y_g|$ by a mooring cable [11].

The incident point of the light propagation path on the water surface is denoted by E with coordinates (x_e, y_e). According to Snell's law [12], the relationship between the incident angle $\theta_{\rm i}$ and the refraction angle $\varphi_{\rm i}$ is given by:

$$n_a \sin(\theta_{\rm i}) = n_w \sin(\varphi_{\rm i}), \tag{3}$$

where $n_a = 1$ and $n_w = 1.333$ are the refractive index of air and water, respectively. The angles $\theta_{\rm i}$ and $\varphi_{\rm i}$ can be calculated by utilizing the slopes of lines $\overline{\rm SE}$ and $\overline{\rm EG}$ and the normal line at the incident point E as follows:

$$\theta_{\rm i} = \tan^{-1}\left|\frac{[y_s - f(x_e,t)]\frac{\partial f(x_e,t)}{\partial x_e} + (x_s - x_e)}{(x_s - x_e)\frac{\partial f(x_e,t)}{\partial x_e} - y_s + f(x_e,t)}\right|, \tag{4}$$

$$\varphi_{\rm i} = \tan^{-1}\left|\frac{[y_g - f(x_e,t)]\frac{\partial f(x_e,t)}{\partial x_e} + (x_g - x_e)}{(x_g - x_e)\frac{\partial f(x_e,t)}{\partial x_e} - y_g + f(x_e,t))}\right|. \tag{5}$$

Substituting (4) and (5) into (3), we can solve (3) for x_e and then obtain $y_e = f(x_e, t)$ based on (1). When there are several solutions of x_e from solving (3), the proper solution is selected by checking whether or not the resulting slopes of lines $\overline{\rm SE}$ and $\overline{\rm EG}$ and the normal line at the incident point E are reasonable for light refraction. Substituting the proper x_e into (4) and (5), we can obtain $\theta_{\rm i}$ and $\varphi_{\rm i}$.

The transmission distances above the water and underwater, the angle β between the optical axis of the LED and the light propagation direction above the water, as well as the angle ϕ between the underwater light propagation direction and the optical axis of the receiver, can be calculated respectively by:

$$|{\rm SE}| = \sqrt{(x_e - x_s)^2 + (y_e - y_s)^2}, \tag{6}$$

$$|{\rm EG}| = \sqrt{(x_e - x_g)^2 + (y_e - y_g)^2}, \tag{7}$$

$$\beta = \tan^{-1}\left|\frac{x_e - x_s}{y_e - y_s}\right|, \tag{8}$$

$$\phi = \tan^{-1}\left|\frac{x_e - x_g}{y_e - y_g}\right|. \tag{9}$$

Other cross sections of the air-to-water communication environment can be obtained by rotating the cross section in Fig. 1 horizontally for an angle in the range from 0 to 180 degrees [8]. The water surface elevation function in the cross section that is rotated around the line of $x = x_s$ from the cross section containing $f(x, t)$ by an angle of r is given by:

$$f(x', t) = f[x\cos(r), t], \tag{10}$$

where $x' = x\cos(r)$. The light propagation path in each new cross section can be obtained in a way similar to the above.

Let β_{rt} denote the angle between the optical axis of the LED and the light propagation direction above the water in the cross section that contains $f[x\cos(r), t]$, where $r \in [0, \pi]$ and $t \in [0, T_w]$, and let θ denote the angular beamwidth of the LED. If $\max\limits_{r,t}\{\beta_{rt}\} \le \frac{\theta}{2}$, then the underwater receiver locatio is in the light coverage at all times. Otherwise, in some cross sections, the underwater receiver location may be outside the light coverage.

C. Received Light Power

In addition to refraction, the water surface also affects the transmittance due to reflection depending on the incident angle. Letting τ denote the transmittance, it is calculated according to Fresnel's equation [12] by:

$$\tau = 1 - \frac{\left|\frac{n_a cos\theta_{\rm i} - n_w cos\varphi_{\rm i}}{n_a cos\theta_{\rm i} + n_w cos\varphi_{\rm i}}\right|^2 + \left|\frac{n_a cos\varphi_{\rm i} - n_w cos\theta_{\rm i}}{n_a cos\varphi_{\rm i} + n_w cos\theta_{\rm i}}\right|^2}{2}. \tag{11}$$

Turbulence may cause the fluctuation of light intensity, known as scintillation, at the underwater receiver [13]. In this work, we focus on a VLC link operating in a water volume characterized by weak turbulence, where the underwater receiver is located no more than 20 meters beneath the water surface and the dissipation rate of mean squared temperature does not exceed $1\times10^{-8}{\rm K}^2/{\rm s}$, a typical value observed in the Pacific Equatorial Undercurrent region [14]. As shown in Fig. 1 of [13], the scintillation index is nearly zero for any dissipation rate of mean squared temperature below $1 \times 10^{-8}{\rm K}^2/{\rm s}$ and light propagation distances of no more than 20 meters beneath the water surface. Therefore, we assume that the effect of turbulence is neglectable in this work.

With light propagating for a distance $\overline{\rm SE}$ in the air, passing through the air-water interface with transmittance τ, and propagating for a distance $\overline{\rm EG}$ underwater, we can obtain the light intensity I at the underwater receiver according to Beer's law [12] as follows:

$$I = \frac{P_{\rm TX}\tau e^{-k_w|{\rm EG}|}}{2\theta|{\rm SE}|^2}, \tag{12}$$

where $P_{\rm TX}$ is the LED transmit power and k_w is the attenuation coefficient of water that depends on the biological factors of water as well as the light wavelength.

The received power $P_{\rm RX}$ at the receiver is then given by:

$$P_{\rm RX} = IAcos(\phi), \tag{13}$$

where A is the receiving area of the underwater receiver.

D. Underwater Received SNR

The average SNR at the receiver is expressed as [15]:

$$\rho = \frac{\Re^2 P_{\rm RX}^2}{\sigma_n^2}, \tag{14}$$

where $\Re = \frac{\gamma q\lambda}{hc}$ is the responsivity of the photodetector at the receiver, γ is the quantum efficiency of the photodetector at the receiver, $q = 1.6 \times 10^{-19}{\rm coulombs}$ is the elementary charge, λ is the wavelength of the light signal in the water, $h = 6.6261\times10^{-34}{\rm J}$ is Plank's constant, and $c = 2.25257\times10^8{\rm m/s}$

is the speed of light in the water; and σ_n^2 denotes the variance of the received noise that includes the background noise, dark current noise, thermal noise, and shot noise, which are assumed to follow independent zero-mean Gaussian distributions with variance of $\sigma_{\rm BG}^2$, $\sigma_{\rm DC}^2$, $\sigma_{\rm TH}^2$ and $\sigma_{\rm SS}^2$, respectively. Hence, the variance σ_n^2 of the noise term n_i is given by [16]:

$$\sigma_n^2 = \sigma_{\rm BG}^2 + \sigma_{\rm DC}^2 + \sigma_{\rm TH}^2 + \sigma_{\rm SS}^2, \tag{15}$$

$$\sigma_{\rm BG}^2 = 2q\Re A {F_V}^2 B_O T_F W R L_f e^{-k_w|y_g|} B, \tag{16}$$

$$\sigma_{\rm DC}^2 = 2qI_{\rm DC}B, \tag{17}$$

$$\sigma_{\rm TH}^2 = \frac{4k_B T_e F B}{R_L}, \tag{18}$$

$$\sigma_{\rm SS}^2 = 2q\Re P_{\rm RX} B. \tag{19}$$

where F_V is the field of view of the receiver, B_O is the optical filter bandwidth, T_F is the optical filter transmissivity, W is the downwelling irradiance of the sun in $\mathrm{watt/m^2}$, R is the underwater reflectance of downwelling irradiance, L_f is the factor describing the directional dependence of underwater radiance, B is the bandwidth of the received light signal, $I_{\rm DC}$ is the dark current, $k_B = 1.381\times10^{-23}\mathrm{J/K}$ is the Boltzmann's constant, T_e is the equivalent temperature in K, F is the circuit noise figure, and R_L is the load resistance.

E. Channel Capacity

For OOK-NRZ with direct detection at the receiver, the channel capacity in bit/pulse is given by [17]:

$$C'_{\rm OOK} = \frac{\rho}{2}\log_2(e) - \frac{e^{\frac{-\rho}{4}}}{\sqrt{2\pi}}\int e^{\frac{-t^2}{2}}\cosh\left(t\sqrt{\frac{\rho}{2}}\right)\log_2\left[\cosh\left(t\sqrt{\frac{\rho}{2}}\right)\right]dt. \tag{20}$$

Since the OOK-NRZ pulse rate is $1/T_b$ pulse/s, the channel capacity in bit/s is then given by:

$$C_{\rm OOK} = \frac{1}{T_b}C'_{\rm OOK}. \tag{21}$$

We consider that this system performs forward error correction (FEC) using Bose–Chaudhuri–Hocquenghem (BCH) code with a code rate of 0.83, which can reduce the BER from 2×10^{-2} before FEC to lower than 1×10^{-12} afterwards [18]. Accordingly, we set the required target BER for our system at $BER_{\rm req} = 2\times10^{-2}$. The maximum net data rate is $0.83\times C_{\rm OOK}$.

For OOK-NRZ under the impact of zero-mean independent Gaussian noise, the relationship between the BER and the received SNR is given by [15]:

$$BER = \frac{1}{2}\,\mathrm{erfc}\left(\frac{1}{2\sqrt{2}}\sqrt{\rho}\right), \tag{22}$$

where $\mathrm{erfc}(.)$ is the complementary error function. Hence, the required SNR for achieving the target BER is given by:

$$\rho_{\rm req} = 8\left[\mathrm{erfc}^{-1}\left(2BER_{\rm req}\right)\right]^2, \tag{23}$$

where $\mathrm{erfc}^{-1}(.)$ is the inverse complementary error function.

III. UAV Energy Consumption Minimization

Let D denote the total amount of data (in bits) that needs to be transmitted from the LED transmitter to the underwater receiver. For simplicity, the transmission time $t_{\rm TX}$ (s) required for transmitting D bits of data to the underwater receiver is approximately given by:

$$t_{\rm TX} \approx D/(0.83\times C_{\rm OOK}). \tag{24}$$

Let η_p denote the LED's transmission power conversion efficiency, which may change with the transmit power of the LED and is usually given in the LED product specification. The power dissipation of the LED for data transmission is then $P_{\rm TX}/\eta_p$. Thus, the total energy consumption of the UAV during the data transmission time is given by:

$$E_{\rm UAV} = \left(P_{\rm UAV} + \frac{P_{\rm TX}}{\eta_p}\right)t_{\rm TX} = \frac{\left(P_{\rm UAV} + \frac{P_{\rm TX}}{\eta_p}\right)D}{0.83\times C_{\rm OOK}}, \tag{25}$$

where $P_{\rm UAV}$ denotes the propulsion power of the UAV.

Our objective is to minimize the UAV's total energy consumption, which consists of the power used for VLC by the LED and the propulsion power of the UAV when hovering above the water, by optimizing the transmit power of the LED under the following constraints: the underwater receiver is in the light coverage at all times; and the SNR at the underwater receiver is above the required SNR for a given BER.

Therefore, the UAV energy consumption minimization problem is formulated as follows:

$$\min_{P_{\rm TX}} E_{\rm UAV}, \tag{26}$$

$$\text{s.t.}\ \max_{r,t}\{\beta_{rt}\} \le \frac{\theta}{2}, \tag{26a}$$

$$\rho \ge \rho_{\rm req}, \tag{26b}$$

$$P_{\min} \le P_{\rm TX} \le P_{\max}, \tag{26c}$$

where $P_{\min}$ and $P_{\max}$ denote the minimum and maximum transmit power of the LED, respectively. Their values can be obtained from the LED product specification, e.g., [19].

We note that the incident point (x_e, y_e) of the light propagation path on the water surface cannot be obtained from (3) analytically because it returns several solutions and the proper solution needs to be identified by checking whether or not each solution is reasonable for light refraction. Hence, we devise an SQP-based algorithm (Algorithm 1) to numerically solve the optimization problem (26).

In Algorithm 1, lines 1-4 firstly analyse the light propagation path from the LED to the underwater receiver and obtain x_e for the incident point E by using (1), (3)–(5) and (10), then calculate $|\mathrm{SE}|$, $|\mathrm{EG}|$, β and ϕ using (6)–(9) for all the cross sections that rotate around the line of $x = x_s$ from 0° to 180° with an increment step size of Δr, each time instant within a time period T_w of the water wave with an increment step size of Δt, and all possible underwater receiver positions at depth $|y_g|$ with x_g increasing from $x_s - x_0$ to $x_s + x_0$ with a step size of Δx_0, where x_0 denotes the longest distance that the underwater VLC receiver may move away from its default location (x_s, y_g). The above 'for' loops construct a discrete spatial-temporal environment for problem (26). This is because both the received SNR ρ in the objective function (25) and constraint (26b) and β_{rt} in constraint (26a) depend on the light propagation path that may vary in space and time. Line 5 calculates the required SNR ρ_{req} using (23). Lines 6-14 construct the objective function $E_{\text{UAV}}(P_{\text{TX}})$ using (25) under constraints (26a) and (26b). Line 15 calls the minimization function 'fmincon' to obtain the optimized transmit power P_{opt} that minimizes the objective function $E_{\text{UAV}}(P_{\text{TX}})$ under constraint (26c) by using the SQP algorithm. Algorithm 1 runs off-line before the UAV is dispatched.

Algorithm 1 UAV energy consumption minimization

Input: $P_{\min}, P_{\max}, BER_{\text{req}}, T_w, \theta, x_s, x_0$
Output: P_{opt}
1: **for all** r, t, x_g **do**
2: Calculate x_e using (1), (3)-(5), and (10);
3: Calculate $\beta, |\text{SE}|, |\text{EG}|, \phi$ using (6)-(9);
4: **end for**
5: Calculate ρ_{req} using (23);
6: **function** $E_{\text{UAV}}(P_{\text{TX}})$
7: **for all** r, t, x_g **do**
8: Calculate ρ using (14)-(19);
9: **if** $\beta(r,t,x_g) \leq \theta/2$ and $\rho(r,t,x_g) \geq \rho_{\text{req}}$ **then**
10: Calculate $E_{\text{UAV}}(P_{\text{TX}}, r, t, x_g)$ using (25);
11: **end if**
12: **end for**
13: $E_{\text{UAV}}(P_{\text{TX}}) \Leftarrow \underset{r,t,x_g}{\text{mean}}\left[E_{\text{UAV}}(P_{\text{TX}}, r, t, x_g)\right];$
14: **end function**
15: $P_{\text{opt}} \Leftarrow \text{fmincon}\left[E_{\text{UAV}}(P_{\text{TX}}), P_{\text{TX}}, P_{\min}, P_{\max}, \text{SQP}\right];$

IV. Simulation Results

In this section, we present the simulation results to evaluate the performance of the proposed algorithm. In our simulation, we consider the UAV DJI Phantom 4 RTK [20] that has a take-off weight of 1391g, battery capacity of 89.2 Wh and propulsion power of 178.4 W. We choose the blue-green light LED LedEngin's LZ4-00B215, which has a wavelength of 465nm in the air [19] and a wavelength of $(n_a/n_w) \times 465\text{nm} = 349\text{nm}$ in the water [12], and use eight of them in the transmitter. We assume that the power consumption of carrying the LEDs has been included in P_{UAV}.

The values of system parameters used in the simulation are listed in Table I, where most of the parameter values are set following [8], [16]. Table II shows the values of P_{TX} for eight LZ4-00B215 LEDs and the corresponding η_p values according to its specification [19].

Fig. 2 shows the optimized LED transmit power obtained by Algorithm 1 versus the depth of underwater receiver and the attenuation coefficient of water, where the incremental step sizes in Algorithm 1 are set as $\Delta r = 10°$, $\Delta t = 0.1\text{s}$ and $\Delta x_0 = 0.2\text{m}$. From Fig. 2, the optimized LED transmit power increases with the depth of underwater receiver for a given attenuation coefficient of water and increases with the attenuation coefficient of water for a given depth of underwater receiver. The highest optimized transmit power of 30.77W is required for the worst scenario of $|y_g| = 15\text{m}$ and $k_w = 0.4\text{m}^{-1}$.

Fig. 3 shows the UAV energy consumption versus the depth of underwater receiver for the optimized LED transmit power obtained by Algorithm 1 in comparison with two benchmarks:

TABLE I
System parameters [8], [16]

Notation	Parameter	Value
$k\alpha$	Wave steepness	0.4
λ_w	Wavelength of water wave	1.3 m
$\|y_s\|$	Distance from transmitter to surface level	10 m
$\|y_g\|$	Distance from receiver to surface level	10 to 15 m
x_0	Underwater receiver localization accuracy	3 m
$P_{\max}$	Maximum LED transmit power	36.56 W
$P_{\min}$	Minimum LED transmit power	4.48 W
BER_{req}	Required bit error rate	2×10^{-2}
A	Receiving area of the underwater receiver	160 mm^2
k_w	Attenuation coefficient of water	0.25 to 0.4 m^{-1}
θ	LED angular beamwidth	45°
F_V	Field of view of the receiver	50 mrad
W	Downwelling irradiance	1440 W/m^2
R	Reflectance of downwelling irradiance	1.25%
L_f	Directional dependence of radiance	2.9
γ	Quantum efficiency of the detector	0.8
I_{DC}	Dark current of the photodiode	1.226×10^{-9} A
T_e	Equivalent temperature	290 K
F	Circuit noise figure	4
R_L	Load resistance	100 Ω
B	Bandwidth of the received light signal	50 kHz
B_O	Optical filter bandwidth	50 nm
T_F	Optical filter transmissivity	55%
P_{UAV}	UAV propulsion power	178.4 W [20]
D	Total data volume to be transmitted	8 Mbit
λ	Wavelength of light signal in water	349nm [19]
T_b	Bit interval	2×10^{-5}s

TABLE II
Transmit power and power conversion efficiency [19]

Transmit power P_{TX} (W) for eight LZ4-00B215 LEDs	4.48	16	24	30	34.4	36.5
Power conversion efficiency η_p	0.46	0.34	0.28	0.25	0.23	0.22

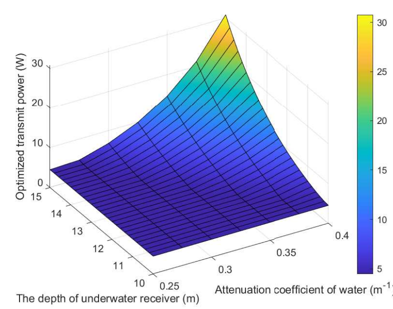

Fig. 2. Optimized transmit power versus the depth of underwater receiver and the attenuation coefficient of water.

LED transmitting at the maximum power which is adopted by [9] and LED transmitting at a random power level uniformly distributed in the range of $[P_{\min}, P_{\max}]$. We can see that the UAV energy consumption with the optimized transmit power obtained by Algorithm 1 is significantly lower than the UAV energy consumption achieved by the two benchmarks at all the considered underwater receiver depths. For the underwater receiver depth of 10 meters, transmitting at the optimized power can save up to 45% of UAV energy consumption as compared with transmitting at the maximum power. The UAV energy consumption for the optimized transmit power and uniformly distributed power schemes increases with the depth of underwater receiver. This is because as the transmission distance increases, the optimized transmit power increases accordingly to maintain

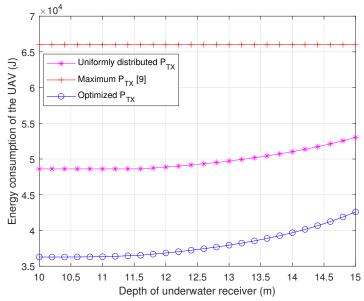

Fig. 3. The energy consumption of the UAV versus the depth of underwater receiver for $k_w = 0.35\text{m}^{-1}$.

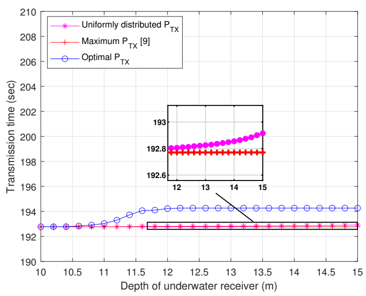

Fig. 4. The required transmission time versus the depth of underwater receiver for $k_w = 0.35\text{m}^{-1}$.

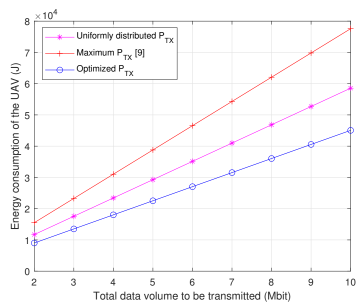

Fig. 5. The energy consumption of UAV versus the total data volume.

a certain transmission rate, while the uniformly distributed power scheme results in a lower transmission rate and requires longer transmission time. The UAV energy consumption under the maximum transmit power remains constant for all the considered depth of underwater receiver, because the maximum transmit power is sufficient to reach the OOK-NRZ channel capacity (and thus a constant transmission rate, transmission time, and UAV energy consumption) for all the considered depth of underwater receiver. This is demonstrated in Fig. 4, which plots the required transmission time versus the depth of underwater receiver for the optimized transmit power and the two benchmarks. From Fig. 4 we can see that transmitting at the optimized power requires only slightly longer transmission time than transmitting at the maximum power, thus resulting in close-to-minimum UAV propulsion energy consumption, while significantly reducing the transmission energy consumption as compared with transmitting at the maximum power.

Fig. 5 shows the energy consumption of UAV versus the total data volume to be transmitted. We can see that the energy consumption gap increases with higher data volume, indicating that the performance improvement achieved by our algorithm is more significant for a higher data volume. This highlights the necessity of optimizing transmit power especially when the data volume is large.

V. Conclusion

In this paper, we have proposed an air-to-water VLC system that includes a comprehensive model of the water surface, light propagation path and various underwater noise terms. Based on the model, we have devised an algorithm to minimize the UAV energy consumption. The simulation results show that the optimized LED transmit power and the energy consumption of the UAV both increase with the depth of the underwater receiver and the attenuation coefficient of water. For the underwater receiver depth of 10 meters, the LED transmit power optimized by the proposed algorithm can reduce the UAV energy consumption by up to 45% as compared to that of LED transmitting at the maximum power.

References

[1] F. S. Alqurashi, A. Trichili, N. Saeed, B. S. Ooi and M. -S. Alouini, “Maritime communications: A survey on enabling technologies, opportunities, and challenges,” *Internet Things J.*, vol. 10, pp.3525-3547, 2023
[2] H. Luo, et al., “Multimodal acoustic-RF adaptive routing protocols for underwater wireless sensor networks,” *IEEE Access*, vol. 7, pp. 134954–134967, 2019.
[3] A. Samir, et al., “Performance analysis of dual-hop hybrid RF-UOWC NOMA systems,” *Sensors*, 22(12), article no. 4521, Jun. 2022.
[4] F. Tonolini and F. Adib, “Networking across boundaries: Enabling wireless communication through the water-air interface,” in *Proc. SIGCOMM*, Aug. 2018, pp. 117–131.
[5] R. S. Sangeetha, R. L. Awasthi and T. Santhanakrishnan, “Design and analysis of a laser communication link between an underwater body and an air platform,” in *Int. Conf. next Gener. Intell. Syst.*, 2016, pp. 1-5.
[6] H. Luo, J. Wang, F. Bu, R. Ruby, K. Wu and Z. Guo, ”Recent progress of air/water cross-boundary communications for underwater sensor networks: A review,” *Sensors J.*, vol. 22, pp. 8360-8382, 2022.
[7] L. E. M. Matheus, et al., ”Visible light communication: concepts, applications and challenges,” *IEEE Commun. Surv. Tut.*, vol. 21, no. 4, pp. 3204-3237, 2019.
[8] M. S. Islam and M. F. Younis, “Analyzing visible light communication through air-water interface,” *IEEE Access*, 7:123830-123845, 2019.
[9] N. Huang, et al., ”Preliminary investigation of air-to-water visible light communication link under strong ambient light,” *VTC*, 2021, pp. 1-5
[10] M. Davies and A.K. Chattopadhyay, “Stokes waves revisited: Exact solutions in the asymptotic limit,” *Eur. Phys. J. Plus*, 131(69), 2016.
[11] S. -M. Yoon, et al.,“Pitch and depth keeping of moored-type underwater acoustic array system,” in *OCEANS*, Seattle, WA, USA, 2019, pp. 1-4.
[12] M. Born, E. Wolf, *Principles of Optics*, Cambridge, U.K.: Cambridge Univ. Press, 1999.
[13] Y. Ata and Y. Baykal, “Scintillations of optical plane and spherical waves in underwater turbulence,” *JOSA A*, vol. 31, pp. 1552-1556, 2014.
[14] S. A. Thorpe, *The Turbulent Ocean*, NY: Cambridge Univ. Press, 2005.
[15] A. M. Ibrahimy, B. I. Fadilah and B. Pamukti, “Analysis of modulation performance of underwater visible light communication with variable wavelength,” in *Int. Conf. Inf. Commun. Technol.*, 2020, pp. 451-455.
[16] S. Jaruwatanadilok, “Underwater wireless optical communication channel modeling and performance evaluation using vector radiative transfer theory,” *IEEE J. Sel. Areas Commun.*, vol. 26, pp. 1620-1627, 2008.
[17] J. S. Everett, “Forward-error correction coding for underwater free-space optical communication,” M.S. thesis, Dept. Elect. Eng., North Carolina State Univ., Raleigh, North Carolina, 2009.
[18] Mizuochi, T. et al., “Next generation FEC for optical transmission systems,” in *OFC*, 2003, vol. 2, pp. 527-528.
[19] LedEngin. *High luminous efficacy blue power LedFlex™ emitter LZ4-00B215*. Accessed: Feb. 11, 2024. [Online]. Available:https://www.farnell.com/datasheets/87098.pdf.
[20] DJI. *Phantom 4 RTK Specs*. Accessed: Feb. 11, 2024. [Online]. Available: https://www.dji.com/gr/phantom-4-rtk/info.